

This paper was presented at a colloquium entitled “Physics: The Opening to Complexity,” organized by Philip W. Anderson, held June 26 and 27, 1994, at the National Academy of Sciences, in Irvine, CA.

The old problems of glass and the glass transition, and the many new twists

C. A. ANGELL

Department of Chemistry, Arizona State University, Tempe, AZ 85287-1604

ABSTRACT In this paper I review the ways in which the glassy state is obtained both in nature and in materials science and highlight a “new twist”—the recent recognition of polymorphism within the glassy state. The formation of glass by continuous cooling (viscous slowdown) is then examined, the strong/fragile liquids classification is reviewed, and a new twist—the possibility that the slowdown is a result of an avoided critical point—is noted. The three canonical characteristics of relaxing liquids are correlated through the fragility. As a further new twist, the conversion of strong liquids to fragile liquids by pressure-induced coordination number increases is demonstrated. It is then shown that, for comparable systems, it is possible to have the same conversion accomplished via a first-order transition within the liquid state during quenching. This occurs in the systems in which “polyamorphism” (polymorphism in the glassy state) is observed, and the whole phenomenology is accounted for by Poole’s bond-modified van der Waals model. The sudden loss of some liquid degrees of freedom through such weak first-order transitions is then related to the polyamorphic transition between native and denatured hydrated proteins, since the latter are also glass-forming systems—water-plasticized, hydrogen bond-cross-linked chain polymers (and single molecule glass formers). The circle is closed with a final new twist by noting that a short time scale phenomenon much studied by protein physicists—namely, the onset of a sharp change in $d\langle r^2 \rangle / dT$ ($\langle r^2 \rangle$ is the Debye–Waller factor)—is general for glass-forming liquids, including computer-simulated strong and fragile ionic liquids, and is closely correlated with the experimental glass transition temperature. The latter thus originates in strong anharmonicity in certain components of the vibrational density of states, which permits the system to access the multiple minima of its configuration space. The connection between the anharmonicity in these modes, vibrational localization, the Kauzmann temperature, and the fragility of the liquid is proposed as the key problem in glass science.

The study of viscous liquids and the glassy state has become increasingly popular since Anderson’s review of the field in 1978 (1) and particularly since the mode-coupling theory (MCT) for viscosity divergence was presented in 1984 (2). It is now recognized as one of the most significant unsolved problems in condensed matter physics and consequently has provoked increasingly sophisticated experimental study and the involvement of an increasing number of theorists. In addition to the existence of new theoretical predictions (3), new aspects of the phenomenology have recently come into focus. For instance the damping of the little understood “boson peak”, believed by many to originate in some inter-

mediate range order (4), has been found (5–7) to correlate with the temperature dependence of the viscosity (i.e., with the so-called “fragility” of the liquid or polymer). At the same time, the notion that a given liquid on slow cooling at constant pressure always tends toward the same conformational ground state has recently been overturned by the recognition of the existence of polymorphism in the glassy state (8–11) [called “polyamorphism” (12)]. Thus the field is in a state of flux. It is an exciting period, as Anderson has opined (13), that a theory of the nature of glass and the glass transition is the “deepest and most interesting unsolved problem in solid state theory.”

Many of the problems in this field are encountered at such long relaxation times as to be “safe” from resolution by the method of molecular dynamics computer simulation (14), though the behavior of real systems near the critical temperature (ideal dynamical glass transition temperature) of MCT is within range. This is certainly also true of the boson peak, which is a short time scale phenomenon; hence, elucidation of the short time dynamics may be expected in the near future. Indeed some progress in this domain is being reported currently (15–17) and will be briefly described herein. In this article, both old and new aspects of the problem are reviewed.

The transition between the configurationally labile liquid, or rubbery, state and the configurationally rigid glassy state is a phenomenon of very broad importance in the physical and materials sciences and in biology. It is, of course, the manner in which the optically isotropic materials of ubiquitous importance in optics are prepared, but it is also, rather less obviously, the strategy by which nature protects vital organisms against harsh environmental conditions (seeds and desert insects against drought, Arctic insects against deep freezing). It is also the strategy mankind uses in the preservation of foodstuffs by desiccation or freezing processes.

This article is condensed from a more detailed paper (16) for the proceedings of the recent Conference on Scaling Concepts in Complex Systems.* As in that case, I will mention the various routes to the glassy state of matter, highlighting the evidence for polyamorphism. Then we will explore in more detail the “normal” route to the glassy state (namely, the cooling of an initially liquid state) and consider the variations in the way liquids slow down as the temperature decreases. In the cases of substances where more than one major amorphous form can be identified, it will be seen that, on cooling, the transformation from one form to another may be observed as a liquid-state transition phenomenon. Since the origin of such an astonishing event is not obvious, its explanation by means of a recent simple thermodynamic model obtained by modifying the van der Waals equation, recently developed by Poole *et al.* (18), will be summarized.

Abbreviation: MCT, mode-coupling theory.

*Conference on Scaling Concepts in Complex Systems, June 28–July 6, 1994, Catanzano, Calabria, Italy.

The publication costs of this article were defrayed in part by page charge payment. This article must therefore be hereby marked “advertisement” in accordance with 18 U.S.C. §1734 solely to indicate this fact.

I will refer briefly to the relation of this phenomenology to the dynamics of hydrated proteins, and particularly the unfolding transition, before closing with some notes relating the very short-time dynamic features of proteins to similar features in simple systems and identifying these as a basis for reconsideration of the basic nature of the glass transition.

Diverse Routes to the Glassy State and Polyamorphism

While the glassy state is conventionally obtained by the cooling of a liquid, it is well known that many alternative routes, such as vapor-phase deposition, desolvation, and *in situ* chemical reaction, are available and in most cases were practiced by nature before materials science took over. The most recently recognized method of amorphization is the least obvious—amorphization by steady compression of open-structured crystals (8–12); a related method is by decompression of extremely compact high-pressure stable crystals (19, 20). The many alternative processes are summarized in Fig. 1.

After a suitable annealing procedure, it is found that the glassy state realized for a given substance by any one of a selection of these methods is remarkably close to that produced by any other, implying that the glassy state exists in a rather well-defined “pocket” in configurational space. However, in certain cases, the glassy state may, in fact, occupy *more than one* distinct pocket, constituting an important “new twist.” It now seems that polyamorphism (12) is a reality. Mishima *et al.* (8–11), who first recognized the process of compression vitrification, also showed that the vitreous form obtained in the initial compression is of very high density compared to the normal vitreous ice. They observed that the normal vitreous ice is produced via a rather sudden relaxation on annealing of the high-density form. Furthermore, the low-density form thus obtained could be returned to the high-density form by something akin to a first-order transition, on recompression, albeit with a large hysteresis, which has a natural explanation. Mishima’s latest work confirms it (11).

This process has been followed spectroscopically in the cases of vitreous SiO₂ and GeO₂ (12). The hysteretically reversible spectral changes have been directly correlated with reversible coordination number changes in the glass by an ion dynamics computer simulation study of the spectral changes associated with polyamorphism in the analogous vitreous BeF₂ system (21). The most careful computer simulation study of the phenomenon, that performed on vitreous ice (22), showed that the low-density amorphous state resists compression up to some critical pressure, which depends on the temperature, whereafter a rapid collapse to a high-density, high-coordination state is observed. It has a well-defined limit that, on being reached, gives rise to a new regime of low compressibility, now characteristic of the high-density amorphous form. The process is reversible with large hysteresis as described in ref. 22, but a small negative pressure is needed to complete the return to the low-density form in the case of H₂O (8–10). A detailed laboratory study with results strikingly supportive of the simulations has recently been published by Mishima (11). A number of cases of polyamorphism have now been discov-

ered and are the subject of much interest in the recent literature.

Later I will relate this phenomenon to the equally important matter of liquid–liquid transformations, after first discussing the basic phenomenology of glass formation by viscous slowdown.

Glass Formation by Viscous Slowdown: Strong and Fragile Liquids and Systems That Can Be Both

Glasses are normally prepared by the steady cooling of an initially liquid state, often followed by an annealing stage in which stresses induced during the vitrification are removed. It is the viscous slowdown process that has been most intensively studied among the various routes to the glassy state and to which I also give most attention.

The glassy state is entered when the cooling liquid passes through the “glass transition,” which is actually a range of temperatures over which the system “falls out of equilibrium.” It is manifested most directly by the systematic decrease of heat capacity from liquid-like to crystal-like values. This abrupt change in the heat capacity, usually amounting to 40–100% of the vibrational heat capacity (i.e., the heat capacity below T_g), is regarded by most workers as the primary signature of the transition between ergodic and nonergodic states. It is illustrated in Fig. 2 for various representative systems. One observes in Fig. 2 that the relative change in heat capacity differs greatly among different systems. Interestingly enough, of the primeval examples of the glassy state (16, 17), three key members (glassy water, vitreous silica, and amber) lack any pronounced thermal signature of the passage from glass to liquid on heating. It will be shown that this casts vitreous water, pure silica, and heavily cross-linked organic resins among the examples of “strong glass formers,” which lie at one extreme of the range of viscous liquid behaviors.

There has been controversy in the literature concerning the fundamental nature of the laboratory glass transition. The controversy centers on the extent to which thermodynamics is relevant to the observed process (23–26). While the process observed in the laboratory is undoubtedly kinetic in origin, it remains unclear whether or not the kinetic phenomenon is underlain by some singularity (1, 23–26) [e.g., a thermodynamic transition of second order, or even first order (27)]. I will make some remarks on this issue later, but for the present purposes it is only necessary to consider the kinetic aspects.

To address the problem of viscous slowdown, it is natural to examine as broad a spectrum of kinetic data as are available and to seek some pattern that might simplify consideration of the problem. A great many viscosity data are available, and it has been found (28–31) that by scaling temperature in an Arrhenius plot by the glass transition temperature itself, the reduction of all data into a comprehensible pattern is achieved. This is shown in Fig. 3, which has been accorded a lot of attention. However, the choice of $T_{(\log \eta=13)}$ as the scaling temperature is not necessarily the best choice. Alternatives based on (i) the glass transition temperature defined by scanning calorimetry at a standard rate and (ii) the temperature at which certain relaxation times reach 10^2 s have also

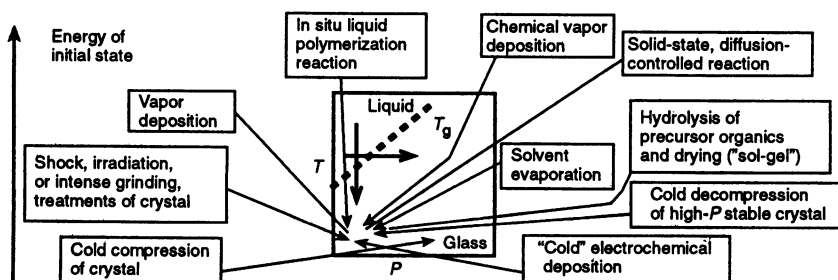


FIG. 1. Various routes to the glassy state, roughly indicating the energies of the initial states relative to the final glassy states. The route of crystal compression below the glass transition temperature (T_g) may yield glasses that are thermodynamically distinct from those obtained by the other route but that may transform to them via nonequilibrium first-order transitions. [Reproduced with permission from ref. 17 (copyright American Association for the Advancement of Science).]

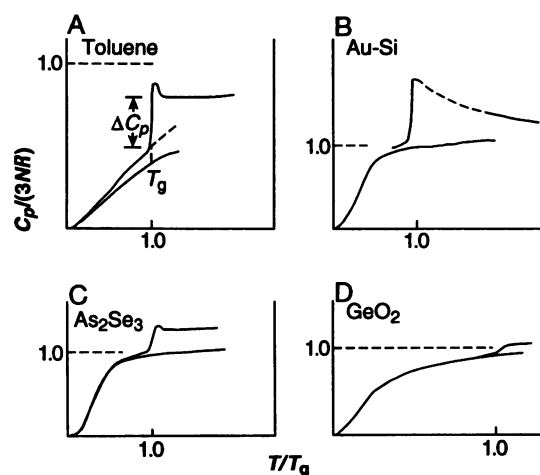


FIG. 2. Heat capacity forms for liquid and crystal phases of different types of substance. (A) Molecular systems like toluene where the glass transition occurs in a range where the crystal heat capacity is not classical. (B) Metallic systems like Au-Si where crystal and liquids reach the classical regime before the glass transition occurs. (C) Covalent systems like As_2Se_3 where the liquid heat capacity jump occurs on a classical background and ΔC_p remains large above T_g . (D) Open network systems like GeO_2 where ΔC_p is small and occurs on a classical background. [Reproduced with permission from ref. 17 (copyright American Association for the Advancement of Science).] $3NR$, classical C_p per mole of heavy atoms.

been utilized (30, 31). While the patterns obtained according to such choices differ in some detail, the broad aspect is unchanged. The almost universal departure from the familiar Arrhenius law, which governs so many rate processes in nature, is the first and arguably the most important canonical feature of glass-forming liquids.

The figure suggests that certain types of liquids form extremes on the general behavior. Open network liquids like SiO_2 and GeO_2 show an Arrhenius variation of the viscosity (or structural relaxation time) between the glass-transition tem-

perature and the high temperature limit and preserve the "strong" liquid extreme of the pattern. Others, characterized by simple nondirectional Coulomb attractions or by van der Waals interactions in a subgroup of substances with many π electrons (primarily aromatic substances), provide the other extreme—"fragile" liquids—in which the viscosities vary in a strongly non-Arrhenius fashion between the high and low limits. This pattern, which has been discussed in some detail previously (29–31), has become known as the strong/fragile liquids pattern and has been used as the basis for a classification of liquids utilizing the same terms. The terms have been chosen to indicate the sensitivity of the liquid structure to change of temperature. The fragile liquids are those whose glassy state structures are teetering on the brink of collapse at their T_g values and that, with little provocation from thermal excitation, reorganize to structures that fluctuate over a wide variety of different structural arrangements and coordination states. Strong liquids, on the other hand, have a built-in resistance to structural change, and their vibrational spectra and radial distribution functions show little reorganization despite wide variations of temperature. Strong liquids can be converted to more fragile behavior by changing their densities—an example will be given below.

The whole pattern can be reproduced quite well by variation of one parameter in a modified version of the famous Vogel–Fulcher–Tammann (32, 33) equation. The original equation

$$\eta = \eta_0 \exp(B/(T - T_0)) \quad [1]$$

is written in the form

$$\eta = \eta_0 \exp(DT_0/(T - T_0)). \quad [2]$$

In this form it is the parameter D , which controls how closely the system obeys the Arrhenius law ($D = \infty$, or $T_0 = 0$). As D changes, so will the value of T_0 change relative to T_g ; the relation is a simple linear one of the form

$$T_g/T_0 = 1 + D/(2.303 \log \eta_g/\eta_0), \quad [3]$$

where $\log(\eta_g/\eta_0)$ is ≈ 17 , according to Fig. 3.

The most fragile liquids identified to date are polymeric in nature, and because of this they cannot be entered into a figure like Fig. 3 without modification. This is because the viscosity of a polymer liquid is largely controlled by its molecular weight (34–36), and this effect must be removed before any common pattern can be obtained. It is necessary in classifying polymer liquids and rubbers to utilize some relaxation time characteristic of the segmental motions (i.e., a microscopic relaxation time, such as is obtained from transient mechanical spectroscopy near T_g , digital correlation spectroscopy, or dielectric relaxation). When this is done, it is found (31, 37) that polycarbonates and polyvinyl chloride are the most fragile systems yet identified with $D \approx 2$. Much more fragile behavior is to be found in certain spin glass systems [e.g., Cu-Mn (38)]. In this case Eq. 3 shows that T_g and T_0 will almost coincide, which is probably the reason for suggestions that in some spin glass systems there is a real phase transition with an associated diverging length scale. The question of an underlying phase transition in viscous liquid systems has been much debated since Kauzmann drew attention to an impending entropy catastrophe in supercooling liquids in his famous 1948 review (26) and is still unresolved. Brief reference to this well-known problem will be made below.

Eq. 2 is by no means the only way of describing the temperature dependence of viscosity or relaxation times in viscous liquids, and many others with three or fewer parameters have been proposed, some with theoretical bases. These are summarized and referenced in ref. 12. It is clear that none can fit precise data over the whole 15 orders of magnitude for

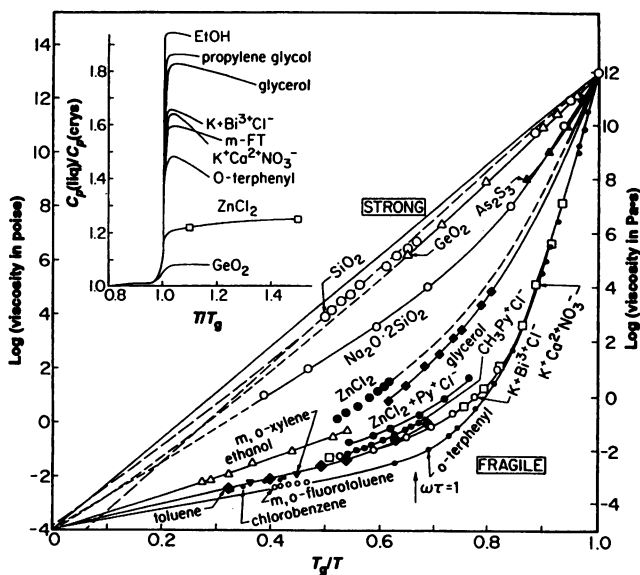


FIG. 3. T_g -scaled Arrhenius plots of viscosity data showing the "strong/fragile" pattern of liquid behavior on which the liquids classification of the same name is based. (Inset) The jump in heat capacity at T_g is generally large for the fragile liquids and small for strong liquids, though there are a number of exceptions to this generalization, particularly when hydrogen bonding is present. (Reproduced from ref. 29.)

which it is available in some cases; indeed, this is not a reasonable expectation unless one has additional parameters as justified in the Cohen–Grest treatment (27). Eq. 2 has the unique advantage that fits of relaxation data near T_g usually give physically appealing (phonon-like) preexponents and T_0 values that agree with the Kauzmann temperatures T_K obtained from purely thermodynamic measurements (26, 39). The theoretical connection may be made through the Adam–Gibbs theory for kinetic processes in cooperative systems (40), which leads to the relation

$$\eta = A \exp(C/TS_c), \quad [4]$$

where S_c is the configurational entropy at temperature T . This yields Eq. 1 if the functional form assumed for excess heat capacity ΔC_p in evaluating S_c [$S_c = \int_{T_K}^T (\Delta C_p/T) dT$] is taken to be $\Delta C_p = K/T$, which is a good approximation to the experimental findings (41, 42). The form the heat capacity would take at temperatures well below T_g , where laboratory studies are impeded by the long time scales, is an open question. Three possibilities that are consistent with the excess entropy remaining at T_g in the carefully studied case of $\text{H}_2\text{SO}_4 \cdot 3\text{H}_2\text{O}$ (43) are illustrated in Fig. 4. Two of them imply phase transitions while the remaining one implies only an anomaly—an exaggerated type of Schottky anomaly (44).

An analysis of the higher temperature, lower viscosity data, which has gained much credence in recent years, is based on the very detailed predictions of MCT. This is described by its authors (2, 3) as a mathematical theory of the glass transition (3), and, as such, much of the physical picture has had to be put in *a posteriori* and there has been some confusion in nomenclature as a result. However, its success in detailing subtle aspects of the phenomenon in the simple atomic systems (45) to which it might be expected to apply [and also to many more complex systems to which application is less expected (26)] is by all accounts remarkable. In this theory, at least in its more tractable versions in which activated processes play no role (2), thermodynamics has no direct role to play. The theory in its idealized version requires the liquid to jam dynamically into a glassy state at temperatures far above T_g and in some cases above T_m , while a fast relaxation mode [which bears no relation to the familiar Johari–Goldstein β -relaxation (46)] continues to be active in the glassy state. The jamming is in practice avoided by the intervention of activated processes, which, for time scales longer than nanoseconds, offer an alternative and more efficient way of relaxing stress to that dealt with by the idealized theory. The “hopping” processes are incorporated in a more advanced form of the theory (3), but this form is highly parameterized, and the predictive prowess in the hopping domain is less marked. Yet it is in this domain that techno-

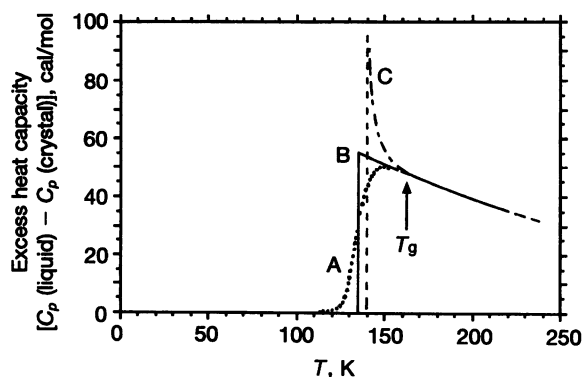


FIG. 4. Alternative heat capacity vs. temperature forms for the case of $\text{H}_2\text{SO}_4 \cdot 3\text{H}_2\text{O}$ (Giaque), which are consistent both with the observable values above T_g and with the condition that the excess entropy of amorphous phase over crystal remain positive or zero down to 0 K.

logically important processes such as refractive index stabilization and physical aging constitute important problems to be solved. In this low-temperature regime, the “fast” process of MCT (i.e., the process associated with anharmonic prediffusion behavior, which is taken up in the last section) remains relevant since barrier crossing must also be preceded by anharmonic cage rattling. However now it is the physics of exploration of the energy landscape, missing from MCT [or introduced somewhat ad hoc as hopping processes, or subsidiary “current” modes (13), to explain the missing singularity], which must be dealt with in detail to understand the slow process. In this sense, as pointed out before (30), MCT only advances the field to the edge of the real problem.

A general interpretation of the pattern of low-temperature, high-viscosity behavior seen in Fig. 3 can be made in terms of the character of the $(3N + 1)$ dimensional energy hypersurface discussed originally by Goldstein (46) and Gibbs (47), discussed more quantitatively by Anderson (1), and now greatly refined by Stillinger and Weber (48, 49). In his classic 1969 paper, Goldstein (46) argued by three different routes that, at viscosities in excess of some 10^2 poise (relaxation times of some 10^{-9} s), corresponding to temperatures of about 1.3 – $1.7 T_g$ (i.e., near the MCT T_c), the liquid structure would be sufficiently coherent to store energy on short time scales and that transport processes would then become activated in some sense. Gibbs envisaged a hypersurface with fewer minima at lower energies (so that the slowing down of the equilibration time with decreasing temperature in proportion to the corresponding decrease in excess entropy S_c could be understood) and one lowest minimum into which the system would settle at the Kauzmann temperature if internal equilibrium were maintained (i.e., at infinitely slow cooling rate).

I have discussed elsewhere (29, 30) the topological features of the hypersurface that would differentiate between strong and fragile liquids and will not repeat the discussion here (although the hypersurface will later be invoked to incorporate the new twist of polyamorphism). Rather, I will note a very new twist to the interpretation of viscous slowdown, which attributes the phenomenology to a singular point at a temperature even higher than that of MCT. Kivelson *et al.* (50) have suggested that the accelerating increase in temperature dependence of viscosity, which sets in at moderate supercooling, or even in the stable state in some pure substances and many solutions, is a consequence of the narrow avoidance of a singularity associated with most favorable packing of the particles. This is not the normal crystalline packing but the extended packing of small clusters (e.g., the tetrahedra in the case of hard spheres), which is only attainable in curved space. The effect of real space frustration of this extended packing order leads to a temperature dependence of the response functions, which is consistent with the viscosities of all the known glass formers (50). The details of the theory, and the physical interpretation of its parameters, remain to be articulated.

It is perhaps consistent with the latter ideas that in the case of strong liquids (which are always the least closely packed) the fragility, which must be interpreted in terms of how narrowly the critical point is avoided, can be strongly affected by changes of density. As hinted at in earlier work (51), and now confirmed by the extended calculations presented in refs. 15 and 16, liquid SiO_2 becomes strongly non-Arrhenius (i.e., much more fragile in the Fig. 3 sense) on compression to $\approx 70\%$ of its normal volume. Whether or not fully fragile behavior can be obtained at higher compression remains to be seen.

In terms of the earlier energy landscape interpretations of viscous slowdown, which I admit to preferring over the avoided critical point proposal, these latter results would imply that a given hypersurface may have regions corresponding to different particle densities, which are characterized by very different densities of minima (see below). These results suggest that a

rigid ion system like BeF_2 (52) or SiO_2 could provide a fruitful subject for theoretical investigations of the hypersurface topologies, which relate alternatively to strong and fragile behavior in liquids. What remains to be shown is that in certain interesting cases these regions with different topologies must be characterized as separate megabasins in the configuration space of a single substance. The megabasins in these cases are separated by major energy barriers such that the system can, under the right circumstances, execute transitions between them; these transitions have the characteristics of first-order phase transitions. For instance, this is necessary to account for the polyamorphic transition seen to occur under nonergodic conditions, in the case of vitreous water described in our first section. Now I show that such transitions may occur in the metastable liquid state, where, at least in principle, the transition can be a reversible phenomenon.

Fragile to Strong Liquid Conversions by First-Order Transition

Fig. 5 shows the microstructure of a quenched melt in the $\text{Y}_2\text{O}_3\text{-Al}_2\text{O}_3$ system reported recently (54). The structure shows droplets of one glass phase embedded in the matrix of another glass. What is remarkable (54) is that the two glassy phases are of identical composition. Only the densities are different. The droplet phase, which must have nucleated and grown from the matrix during the quench, is the low-density and low-entropy phase. The inevitable conclusion is that a first-order transition from a high-density liquid to a low-density liquid occurred during the quench but was arrested before it could be completed because of the fast quench and the highly viscous condition under which the nucleation was initiated. The high-temperature liquid, according to the available viscosity data and the best estimate of the glass transition temperature of the droplet phase, is a very fragile liquid, so it is not unreasonable to suppose that the transition is also one from a fragile to a strong liquid.

This is entirely consistent with what had already been suggested (55) for the behavior of pure water during quenches so rapid that the glassy state is obtained (56). The latter requires exceptionally fast cooling as the boiling point-to-melting point ratio for water is only 1.36:1. It is well documented for water that both the thermodynamic and the transport properties approaching -45°C become highly anomalous (57, 58) and comparable to those of some liquid crystals approaching their weakly first-order mesophase transitions

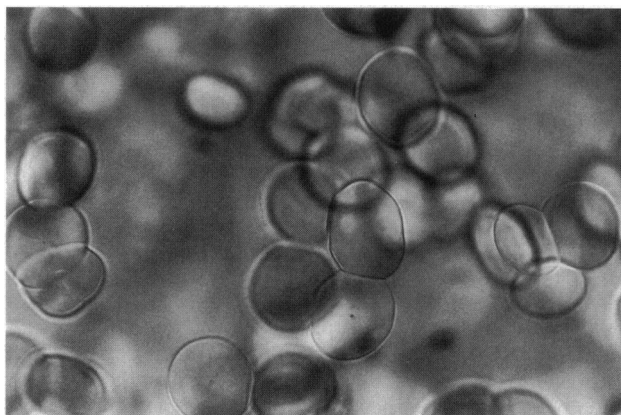


FIG. 5. Microstructure showing two glassy phases of identical composition formed by quenching an initially homogeneous oxide melt in the system $\text{Y}_2\text{O}_3\text{-Al}_2\text{O}_3$. The droplet phase is found to be of lower density and has evidently nucleated from the denser phase, which is a fragile liquid at 2000 K (Fig. 3), during the quenching. Faster cooling suppresses the formation of the droplet phase (54). [Reproduced with permission from ref. 54 (copyright Macmillan Magazines).]

(59). The anomalies are a consequence of approach to a singularity (I would argue a spinodal instability) near which fluctuations slow down and diverge, which lies shortly below the first-order transition temperature. The low-temperature phase of water is an open network (60, 61) like SiO_2 , and it is not surprising (see Fig. 4) that it should be a strong liquid.

The manner in which such weak first-order transitions can arise in atomic and small molecule liquids prone to open network bonding has been demonstrated in two recent theoretical papers (18, 62), one of them a microscopic model (62). The phase diagrams for two water-like substances with different hydrogen bond strengths obtained from the first of these are shown in Fig. 6 (no crystalline phases). The value of the bond strength determines whether a first-order liquid-liquid transition occurs at all pressures or only at pressures above ambient. Again the low-temperature phase is a low-density, low-entropy phase.

The slopes of the liquid-liquid phase transition lines in Fig. 6 are those expected from the Clapeyron equation and, in combination with the spinodal lines radiating out from the critical point, show why the polyamorphic phase change observed under nonergodic conditions in both laboratory (11) and simulation studies (22) occurs hysteretically (11, 22). The amorphization of certain high-pressure metallic phases transforming to low-density tetrahedral semiconducting glasses on

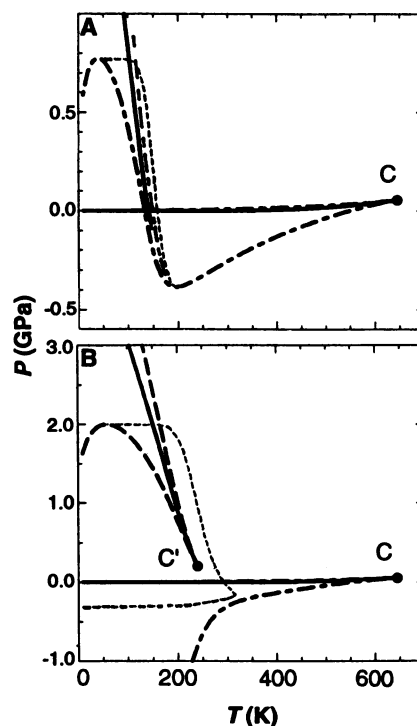


FIG. 6. Phase diagrams from bond-modified van der Waals model for water (18) based on choice of hydrogen bond-breaking energy consistent with spectroscopic evidence, $\Delta H = 14$ kJ/mol (A) and the energy indicated by potential functions used for water simulations, $\Delta H = 22$ kJ/mol (B). For the former parameter choice, the phase diagram is consistent in form with that derived from the Haar-Gallagher-Kell equation of state (63) and suggests a line of liquid-liquid first-order transitions with negative Clapeyron slope running between the liquid vapor spinodal at negative pressure and uncharted regions at high pressure. For the latter parameter choice, the line of first-order transitions terminates at a critical point at moderate pressures, marked C'. This is the result obtained in the computer simulation studies using common pair potentials (see ref. 64). Note the disposition of the spinodal lines above and below the transition line. Approach to a spinodal is accompanied by diverging fluctuations and anomalous physical properties. Dotted lines are loci of density maximum temperatures. [Adapted with permission from ref. 18 (copyright The American Physical Society).]

decompression (53) has been explained using similar phase diagrams (which have second critical points at negative pressures) derived from “two-fluid” models (64).

Other common systems with the same characteristics as water—open tetrahedral network low-temperature amorphous phases and higher density liquids—are silicon and germanium. There are also a variety of like-structured binary compounds such as InSb and CdTe with unusual behavior (65). In the case of silicon, first-order phase transitions between high-density liquid and lower density tetrahedral amorphous (viscous liquid) phases have been observed in computer simulation studies (M. Grabow, personal communication) and have also been reported in very short time scale experiments (66) in which the transition from amorphous network to metallic liquid was called a first-order “melting” transition. This occurred at a temperature well below the normal melting point of the crystal. As with water, the experimental problem impeding study is the ultrafast crystallization of the stable crystal phase during cooling.

To accommodate these new phenomena, a more general version of the hypersurfaces discussed earlier is drawn in Fig. 7. This version permits the low-entropy strong liquid state to be found by first-order phase change (configuration space tunneling) from a fragile (higher entropy) state, which involves nucleation and growth as evidenced in Fig. 5. At low temperatures in the glassy state, the possibility of nucleating a phase change, hence of finding an equilibrium transition, vanishes, but it is still possible for the phase change to occur by a spinodal type mechanism. In this type of mechanism, the system can be moved, by elastic distortions, along a continuous uphill path in the configuration space of one megabasin until an overlap with a minimum in the adjacent megabasin occurs and the system falls into it (see Fig. 7). This path is absolutely irreversible, and the transition on decomposition can only be accomplished by a comparably large elastic distortion in the opposite direction, hence, the large hysteresis demonstrated so definitively in the studies of Mishima (11) and Poole *et al.* (22). Liquid-crystal mesophases, which may be viscous and glass forming (67), can also be represented by hypersurfaces with distinct megabasins. When lines of glass transitions cross mesophase boundaries, polyamorphs, which are distinguished by orientations rather than density, may be obtained (68). The liquid crystal first-order transitions are distinguished from the present cases by being observable as stable state phenomena and by

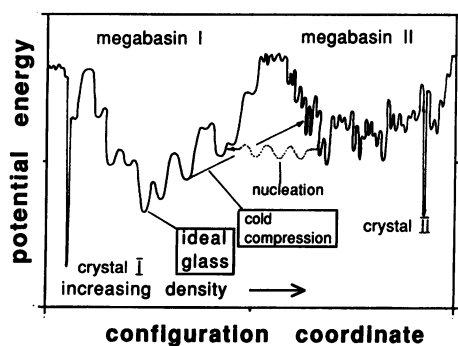


FIG. 7. Potential energy hypersurface showing megabasins needed to understand the existence of polyamorphic forms and the observed first-order-like phase transitions between them. The wavy horizontal arrow indicates narrow channel in configuration space (out of plane of paper) by which nucleation of the low-entropy phase can occur during cooling (strictly, the vertical axis should be a chemical potential in order for the horizontal transition to be appropriate). The inclined straight line schematizes how cold compression can lead to sudden (unnucleated, spinodal-like) collapse to a higher density glass. In addition to the article by Stillinger (49), a good discussion of the nature of the configuration space minima, with an emphasis on spin glasses, is given in an important review of the glassy state by Anderson (1). [Reproduced with permission from ref. 17 (copyright American Association for the Advancement of Science).]

having only very small changes in heat capacity across the transitions. Thus, presumably they cannot be classified as strong \leftrightarrow fragile liquid transitions.

Other Canonical Features of Liquids Near the Glass Transition

The non-Arrhenius behavior described above is only the first of three canonical characteristics of glass-forming liquids. There are two others: (i) the nonexponentiality of relaxation (69–76), most economically described (74) by the parameter β in the Kohlrausch relaxation function,

$$\theta(t) = \exp[-(t/\tau)^\beta], \quad [5]$$

and (ii) the nonlinearity of relaxation (77–82) which, for nonergodic systems, describes the relative importance of pure temperature vs. fictive temperature (81) in determining τ of Eq. 5. The fictive temperature is a convenient way of quantifying the difference between the structure of the fully equilibrated liquid and the structure whose relaxation is being measured. This somewhat complex matter is fully described in a recent review by Hodge (79). For our purposes here, the important point is that the parameters describing these two additional characteristics of relaxing liquids seem to be closely correlated to the corresponding fragilities. The correlation of exponentiality with non-Arrhenius character is an old one (69), which has been refined and qualified recently (73). The correlation of nonlinearity with fragility was until recently dependent on fits of scanning data to multiparameter functions (77–79), but it has now been confirmed by precise isothermal enthalpy relaxation studies (80).

The new twists in this research area have been the discovery of an apparently universal scaling of the relaxation spectra (75), which is consistent with an expectation from percolation theory (71) and the use of universal deviations from Eq. 5 at high f/f_{\max} (75) to argue for a divergent susceptibility at T_0 of Eqs. 1 and 2 (76). Thus T_0 , if it exists, is the temperature of the phase transition. This would suggest that curve C in Fig. 4 may be closest to the mark.

“Glassy” Dynamics and Phase Transitions in Polypeptides and Proteins

It was shown in refs. 16 and 17 that, in the Poole model (18), the low-temperature phase of liquid water has a considerable fraction of its configuration microstates still available to it below the phase transition temperature. The analogy to the *liquid crystal* phase transition phenomenon was made earlier in this paper. Now it seems appropriate to make a further analogy to the transitions in biopolymers from random coil to noncrystalline helical states or alternatively to the more complex native protein states. Here, as in a-Si, most interest lies in the properties of the amorphous substance *below* the phase transition temperature.

The dynamics of processes in native protein molecules have been discussed in terms of glassy dynamics by many authors in recent years (83–96), initially by analogy to spin glasses (83, 84). Indeed, the strongly nonexponential character of the relaxations observed and the absence of a normal C_p jump where the mobility sets in support this analogy. On the other hand, the mobile particles are atoms and molecule groups, not spins (or even on-off bonds), and recent discussions have tended more toward reconciliation of the protein behavior with that of more conventional glass-forming polymeric materials. The absence of a C_p jump has been explained by reference to the behavior of interpenetrating networks by Sartor *et al.* (95) and by intrusion of secondary relaxations (concentrated in the water-side group interactions, which occur mainly at the protein surface) by Green *et al.* (96). Space does not allow examination of this complex issue here. Rather,

I am interested in examining the idea that the folding transition at the high end of the excitation process is generically related to the polyamorphic transition between strong and fragile liquid states discussed earlier. As evidence we show, in Fig. 8 from the work of Sochava and Smirnova (93), how the unfolded protein exhibits a much more pronounced glass transition than its folded relative. Certainly, like water I relative to water II (55), it has much more mobility at the same temperature (90). Furthermore, there is evidence from protein crystal studies (85) that a state of absolute instability (a spinodal) exists just above the unfolding transition as predicted by the Poole model (18) for the polyamorphic transition in simple atomic or molecular systems. This intriguing matter is considered in more detail elsewhere (16, 17).

Anharmonicity and the Glass Transition

Another link between protein dynamics and the behavior of more familiar glasses can be made via the short time dynamics observed in each case. The rather sudden change of slope that occurs in the plot of the Debye–Waller factor [mean square displacement of the system's particles ($\langle r^2 \rangle$)] vs. T in proteins has been called a transition by many protein physicists (85–91) and associated with the glass transition although, as noted above, no C_p jump is seen at this “transition” temperature. Observations based on Mossbauer scattering (85, 97) and neutron scattering studies (98–101) show that the same occurs in simple liquids (98), solutions (ref. 97 and B. Olsen, personal communication), and chain polymers (99–101), and here the slope change temperature indeed more or less coincides with the calorimetric T_g . In one case (ref. 98 and B. Olsen, personal communication), two different Mossbauer nuclei, ^{119}Sn and ^{57}Fe , with different lifetimes were used in the same solution.

In some cases, the break has been attributed to the onset of inelastic processes and interpreted in terms of MCT (98, 99). In ref. 97, the departure from harmonic behavior was interpreted as due to the nonlinearity of the $\langle r^2 \rangle$ vs. time in the pre-diffusional regime. It was shown that the same $\langle r^2 \rangle$ applies to Fe^{3+} and Sn^{4+} ; differences found in the calculated Debye–Waller factors for Sn and Fe at high T correlated with the different Mossbauer lifetimes. In a study of the elemental glass-former, selenium, which is polymeric, Buchenau and Zorn (102) gave an alternative interpretation of the departure from harmonic behavior, based on the concept of soft phonons, and the high temperature $\langle r^2 \rangle$ values were correlated with the viscosity through a treatment analogous to that of Cohen and Turnbull for free volume (103). A number of the observations are collected in Fig. 9. The calorimetric T_g values follow the compound identification in the legend (except for the protein for which no such T_g can be seen), and the

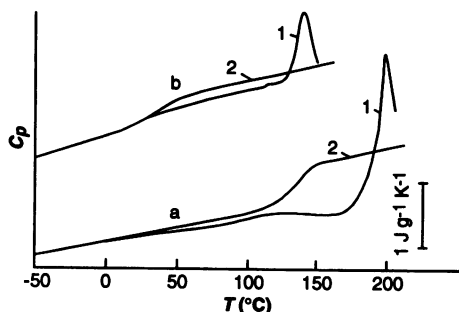


FIG. 8. Differential scanning calorimeter scans of the globular protein legumin both before and after denaturation, for different water contents: curve a, dry; and curve b, 10.4% (wt/wt) water. Note the increase in calorimetric strengths of glass transitions after denaturation. The native state acts like a strong liquid (Fig. 4). [Reproduced with permission from ref. 93 (copyright Oxford University Press).]

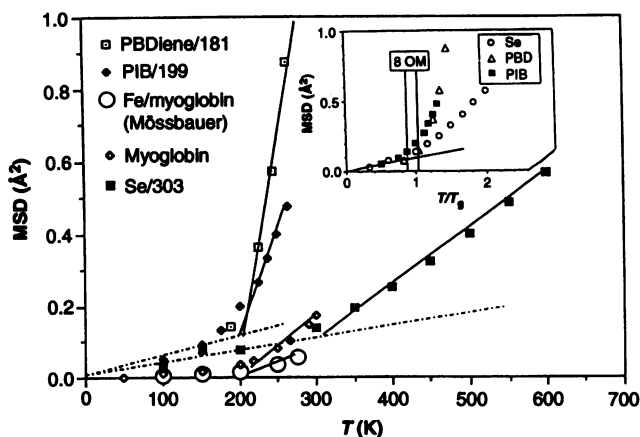


FIG. 9. Variations of the Debye–Waller factor, $\langle r^2 \rangle$, with T_g -scaled temperature, showing the change of slope around the temperature of the calorimetric glass transition, T_g . T_g values in degrees Kelvin are given after the substance identity in the key. (Inset) Same data vs. T/T_g (except for the protein myoglobin for which T_g is only ambiguously defined by calorimetry). The band marked 8 OM shows the reduced temperature range needed to change the relaxation time of a fragile liquid, *o*-terphenyl, by 8 orders of magnitude. [Reproduced with permission from ref. 17 (copyright American Association for the Advancement of Science).]

proximity of the anomaly to T_g may be seen from the T_g -scaled plot of the data shown in Fig. 9 Inset.

Computer simulation studies of $\langle r^2 \rangle$ for strong fragile ionic glass formers of differing bonding topologies, described elsewhere (15–17), show that the break in $\langle r^2 \rangle$ vs. T occurs near the experimental T_g , even in the absence of any diffusive displacements, a result that supports the old suggestion (104) that the glass transition phenomenon originates in strong vibrational anharmonicity in local rearranging groups. This now seems to promote boson mode damping, which is the trigger for the onset of particle diffusion, which, in turn, permits structural relaxation and hence all the other phenomena characteristic of the viscous liquid state.

The implication is that there are subtle connections between very short time dynamic processes, perhaps involving vibrational localization phenomena (105), which are intrinsic to the exchange of energy between vibrational and configurational degrees of freedom [the “phonon–configuron” exchange (104)], hence to the manner in which a many-particle system gains access to the multiple minima of its potential energy hypersurface. These, and the anharmonic couplings that must be involved, must be accounted for before the manner in which glasses regain the quasi-ergodicity of the supercooled liquid state during warming can be properly understood. It is amusing to speculate that the glass transition may in the future find its fundamental interpretation in a heavy particle version of the electron localization phenomenon, which emerged (106, 107) to solve the problem at the center of the last great surge of interest in the phenomenology of the glassy state (the metal-to-semiconductor transition).

Concluding Remarks

The field of viscous liquids and the glass transition has certainly been enriched by recent developments and offers more challenges than ever before. The key problems are those of (i) determining the conditions under which polyamorphism is or is not manifested, contrasting the physical properties of the two glassy states, and clarifying the relation to transitions in biopolymer systems; (ii) determining the general behavior of liquids near their T_g at high pressure (108), where attractive forces will be less important; and (iii) understanding the nature of the boson peak and its damping (and of anharmonicity in

general), how they combine to determine the fragility or otherwise of a given liquid, and whether or not these are all connected through the onset of microheterogeneity in the supercooling liquid structure as it approaches the glass transition.

I acknowledge the support of the National Science Foundation under Solid State Chemistry Grant No. DMR9108028-002 and the help of many colleagues through stimulating discussions of this subject area. In particular, I am grateful to Uli Buchenau, Walter Kob, Paul Madden, Peter Poole, Hans Sillescu, and George Wolf.

1. Anderson, P. W. (1979) in *Ill-Condensed Matter*, eds. Balain, R., Maynard, R. & Toulouse, G. (North-Holland, Amsterdam), Course 3, pp. 162–258.
2. Bengtzelius, U., Götz, W. & Sjölander, A. (1984) *J. Chem. Phys.* **17**, 5915–5924.
3. Götz, W. & Sjögren, L. (1992) *Rep. Progr. Phys.* **55**, 55–77.
4. Martin, A. J. & Brenig, W. (1974) *Phys. Status Solidi* **64**, 163–169.
5. Sokolov, A. P., Kisliuk, A., Soltwisch, M. & Quitmann, D. (1992) *Phys. Rev. Lett.* **69**, 1540–1543.
6. Sokolov, A. P., Kisliuk, A., Quitmann, D. & Kudik, A. (1994) *J. Non-Cryst. Solids* **172–174**, 138–153.
7. Hassan, A. K., Börjesson, L. & Torell, L. M. (1994) *J. Non-Cryst. Solids* **172–174**, 154–160.
8. Mishima, O., Calvert, L. D. & Whalley, E. (1984) *Nature (London)* **310**, 393–395.
9. Mishima, O., Calvert, L. D. & Whalley, E. (1985) *Nature (London)* **314**, 76–78.
10. Mishima, O., Takemura, K. & Aoki, K. (1991) *Science* **254**, 406–408.
11. Mishima, O. (1994) *J. Chem. Phys.* **100**, 5910–5913.
12. Wolf, G. H., Wang, S., Herbst, C. A., Durben, D. J., Oliver, W. J., Kang, Z. C. & Halvorsen, C. (1992) in *High-Pressure Research: Application to Earth and Planetary Sciences*, eds. Manghni, Y. S. & Manghni, M. H. (Terra Scientific/Am. Geophys. Union, Washington), pp. 503–517.
13. Anderson, P. W. (1995) *Science* **267**, 1615–1616 (lett.).
14. Angell, C. A., Clarke, J. H. R. & Woodcock, L. V. (1981) *Adv. Chem. Phys.* **48**, 397–453.
15. Shao, J. & Angell, C. A. (1995) in *Proceedings of the 17th International Congress on Glass*, in press.
16. Poole, P. H., Shao, J. & Angell, C. A. (1995) *Nuovo Cimento* **16**, 993–1007.
17. Angell, C. A. (1995) *Science* **267**, 1924–1935.
18. Poole, P. H., Sciortino, F., Grande, T., Stanley, H. E. & Angell, C. A. (1994) *Phys. Rev. Lett.* **73**, 1632–1635.
19. Liu, L.-G. & Ringwood, A. E. (1975) *Earth Planet. Sci. Lett.* **28**, 209–211.
20. Hemmati, M., Chizmeshya, A., Wolf, G. H., Poole, P. H., Shao, J. & Angell, C. A. (1995) *Phys. Rev. B*, in press.
21. Boulard, B., Angell, C. A., Kieffer, J. & Phifer, C. C. (1992) *J. Non-Cryst. Solids* **140**, 350–358.
22. Poole, P. H., Sciortino, F., Essmann, U. & Stanley, H. E. (1992) *Nature (London)* **360**, 324–328.
23. Gibbs, J. H. & Dimarzio, E. A. (1958) *J. Chem. Phys.* **28**, 373–388.
24. Jackle, J. (1986) *Rep. Progr. Phys.* **49**, 171–188.
25. Angell, C. A., Alba, C., Arzimanoglou, A., Böhrer, R., Fan, J., Lu, Q., Sanchez, E., Senapati, H. & Tatsumisago, M. (1992) *Am. Inst. Phys. Conf. Proc.* **256**, 3–19.
26. Kauzmann, A. W. (1948) *Chem. Rev.* **43**, 219.
27. Cohen, M. H. & Grest, G. (1979) *Phys. Rev. B* **20**, 1077–1086.
28. Laughlin, W. T. & Uhlmann, D. R. (1972) *J. Phys. Chem.* **76**, 2317–2325.
29. Angell, C. A. (1985) in *Relaxations in Complex Systems*, eds. Ngai, K. & Wright, G. B. (Natl. Tech. Inf. Serv., U.S. Dept. Commerce, Springfield, VA), p. 1.
30. Angell, C. A. (1991) *J. Non-Cryst. Solids* **131–133**, 13–31.
31. Angell, C. A., Monnerie, L. & Torell, L. M. (1991) *Symp. Mat. Res. Soc.* **215**, 3–9.
32. Fulcher, G. S. (1925) *J. Am. Ceram. Soc.* **8**, 339–343.
33. Tammann, G. & Hesse, W. Z. (1926) *Anorg. Allgem. Chem.* **156**, 245–256.
34. Ferry, J. D. (1980) *Viscoelastic Properties of Polymers* (Wiley, New York), 3rd Ed.
35. Scherer, G. W. (1992) *J. Am. Ceram. Soc.* **75**, 1060–1061.
36. Wang, C. H., Fytas, G., Lilge, D. & Dorfmueller, T. H. (1981) *Macromolecules* **14**, 1363.
37. Plazek, D. J. & Ngai, K. L. (1991) *Macromolecules* **24**, 1222.
38. Souletie, J. (1990) *J. Phys.* **51**, 883–889.
39. Angell, C. A. (1970) *J. Chem. Educ.* **47**, 583–587.
40. Adam, G. & Gibbs, J. H. (1965) *J. Chem. Phys.* **43**, 139–146.
41. Privalko, Y. (1980) *J. Phys. Chem.* **84**, 3307–3317.
42. Alba, C., Busse, L. E. & Angell, C. A. (1990) *J. Chem. Phys.* **92**, 617–624.
43. Kunzler, J. E. & Giaque, W. F. (1952) *J. Am. Chem. Soc.* **74**, 797–800.
44. Angell, C. A. & Rao, K. J. (1972) *J. Chem. Phys.* **57**, 470–481.
45. Kob, W. & Andersen, H. C. (1984) *Phys. Rev. Lett.* **73**, 1376–1379.
46. Goldstein, M. (1969) *J. Chem. Phys.* **51**, 3728–3741.
47. Gibbs, J. H. (1960) in *Modern Aspects of the Vitreous State*, ed. McKenzie, J. D. (Butterworths, London), Chap. 7, pp. 152–187.
48. Stillinger, F. H. & Weber, T. A. (1982) *Phys. Rev. A* **25**, 978–989.
49. Stillinger, F. H. & Weber, T. A. (1984) *Science* **228**, 983–989.
50. Kivelson, S. A., Zhao, X., Fischer, T. M. & Knobler, C. M. (1994) *J. Chem. Phys.* **101**, 2391–2399.
51. Angell, C. A., Cheeseman, P. A. & Phifer, C. C. (1986) *Mater. Res. Soc. Symp. Proc.* **63**, 85–94.
52. Rahman, A., Fowler, R. H. & Narten, A. H. (1972) *J. Chem. Phys.* **57**, 3010.
53. Poyatovsky, E. G. & Barkalov, O. I. (1992) *Mater. Sci. Rep.* **8**, 147–191.
54. Aasland, S. & McMillan, P. F. (1994) *Nature (London)* **369**, 633–636.
55. Angell, C. A. (1993) *J. Phys. Chem.* **97**, 6339–6341.
56. Mayer, E. J. (1985) *J. Appl. Phys.* **58**, 663–668.
57. Speedy, R. J. & Angell, C. A. (1976) *J. Chem. Phys.* **65**, 851–858.
58. Angell, C. A. (1983) *Annu. Rev. Phys. Chem.* **34**, 593–630.
59. De Gennes, P.-G. & Prost, J. (1993) *The Physics of Liquid Crystals* (Oxford Univ. Press, Oxford, U.K.).
60. Narten, A. H., Venkatesh, C. G. & Rice, J. A. (1976) *J. Chem. Phys.* **64**, 1106–1114.
61. Rice, S. A. & Sceats, M. G. (1982) in *Water: A Comprehensive Treatise*, ed. Franks, F. (Plenum, New York), Vol. 7, pp. 83–211.
62. Borick, S., Sastry, S. & Debenedetti, P. (1995) *J. Phys. Chem.* **99**, 3781–3790.
63. Haar, L., Gallagher, J. & Kell, G. S. (1985) *National Bureau of Standards Research Council Steam Tables* (McGraw-Hill, New York).
64. Aptekar, I. L. (1979) *Sov. Phys. Dokl. (Engl. Transl.)* **24**, 993–999.
65. Glazov, V. M., Chizhevskaya, S. N. & Evgen'ev, S. B. (1969) *Russ. J. Phys. Chem. (Engl. Transl.)* **43**, 201–207.
66. Thompson, M. O., Galvin, G. J. & Mayer, J. W. (1984) *Phys. Rev. Lett.* **52**, 2360–2363.
67. Johari, G. P., Johnson, G. E. & Goodby, J. W. (1982) *Nature (London)* **297**, 315–317.
68. Mirnaya, T. A. & Volkov, S. V. (1994) *Liq. Cryst.* **16**, 687–692.
69. Litovitz, T. A. & McDuffie, G. (1963) *J. Chem. Phys.* **39**, 729–737.
70. Ngai, K. L., Rendell, R. W. & Teitler, R. S. (1986) *Ann. N.Y. Acad. Sci.* **484**, 150–180.
71. Chamberlin, R. V. & Kingsbury, D. W. (1994) *J. Non-Cryst. Solids* **172–174**, 318–326.
72. Ngai, K. L., Rendell, R. W. & Plazek, D. J. (1991) *J. Chem. Phys.* **94**, 3018–3029.
73. Böhrer, R., Ngai, K. L., Angell, C. A. & Plazek, D. J. (1993) *J. Chem. Phys.* **99**, 4201–4209.
74. Alvarez, F., Allegria, A. & Colmenero, J. (1993) *Phys. Rev. B* **47**, 125–131.
75. Dixon, P. K., Wu, L., Nagel, S. R., Williams, B. D. & Carini, J. P. (1990) *Phys. Rev. Lett.* **65**, 1108.
76. Menon, N. & Nagel, S. (1994) *Phys. Rev. Lett.* **74**, 1230–1233.
77. Moynihan, C. T., Chrichton, S. N. & Opalka, S. M. (1991) *J. Non-Cryst. Solids* **131–133**, 420–434.
78. Hodge, I. M. (1991) *J. Non-Cryst. Solids* **131–133**, 435–441.
79. Hodge, I. M. (1994) *J. Non-Cryst. Solids* **169**, 211–266.
80. Fujimori, H., Fujita, H. & Oguni, M. (1995) *Bull. Chem. Soc. Jpn.* **68**, 447–455.
81. Tool, A. Q. (1946) *J. Am. Ceram. Soc.* **29**, 240–252.
82. Narayanaswamy, O. S. (1971) *J. Am. Ceram. Soc.* **54**, 491–502.
83. Goldanskii, V. I., Krupnyanskii, Y. F. & Fleurov, V. N. (1983) *Dokl. Akad. Nauk SSSR* **272**, 978–991.
84. Stein, D. (1985) *Proc. Natl. Acad. Sci. USA* **82**, 3670–3672.
85. Doster, W., Bachleitner, A., Dunau, R., Hiebi, M. & Lüscher, E. (1986) *Biophys. J.* **50**, 213–219.
86. Parak, F., Heidemeier, J. & Nienhaus, G. U. (1988) *Hyperfine Interac.* **40**, 147–157.
87. Iben, I. E. T., Braunstein, D., Doster, W., Frauenfelder, H., Hong, M. K., Johnson, J. B., Luck, S., Ormos, P., Schulte, A., Steinbach, P. J., Xie, A. H. & Young, R. D. (1989) *Phys. Rev. Lett.* **62**, 1916–1919.
88. Frauenfelder, H., Sligar, S. G. & Wolynes, P. C. (1991) *Science* **254**, 1598–1603.
89. Doster, W., Cusack, S. & Petry, W. (1989) *Nature (London)* **337**, 754–756.
90. Rasmussen, B. F., Stock, A. M., Ringe, D. & Petsko, G. A. (1992) *Nature (London)* **357**, 423–424.
91. Smith, J., Kuczera, K. & Karplus, M. (1990) *Proc. Natl. Acad. Sci. USA* **87**, 1601–1605.
92. Sochava, I. V., Tseretoli, G. I. & Smirnova, O. I. (1991) *Biofizika*, 36–40.
93. Sochava, I. V. & Smirnova, O. I. (1993) *Food Hydrocolloids* **6**, 513–524.
94. Morozov, V. N. & Marozova, T. Y. (1993) *J. Biomol. Struct. Dyn.* **11**, 459–461.
95. Sartor, G., Mayer, E. & Johari, G. P. (1994) *Biophys. J.* **66**, 249–258.
96. Green, J. L., Fan, J. & Angell, C. A. (1994) *J. Phys. Chem.* **98**, 13780–13791.
97. Ollsen, B. (1977) *Proc. Int. Conf. Mössbauer Spectrosc.* **7**, 2–2.
98. Petry, A., Bartsch, E., Fujara, F., Kiebel, M., Sillescu, H. & Farrago, B. (1991) *Z. Phys. B. Condens. Matter* **83**, 175–182.
99. Frick, B. & Richter, D. (1993) *Phys. Rev. B* **47**, 14795–14801.
100. Frick, B., Richter, D., Petry, W. & Buchenau, U. (1988) *Z. Phys. B. Condens. Matter* **70**, 73–79.
101. Chahid, A., Allegria, A. & Colmenero, J. (1994) *Macromolecule* **27**, 3282–3288.
102. Buchenau, U. & Zorn, R. (1992) *Europhys. Lett.* **18**, 523–526.
103. Cohen, M. H. & Turnbull, D. (1959) *J. Chem. Phys.* **31**, 1164.
104. Angell, C. A. (1968) *J. Am. Ceram. Soc.* **51**, 117–124.
105. Buchenau, U. (1992) *Philos. Mag.* **65**, 303–315.
106. Anderson, P. W. (1958) *Phys. Rev.* **109**, 1492–1499.
107. Anderson, P. W. (1978) *Rev. Mod. Phys.* **50**, 191–221.
108. Herbst, C. A., Cook, R. L. & King, H. E. (1994) *J. Non-Cryst. Solids* **172–174**, 265–271.